Journal of
Ceramic Science
and Technology

J. Ceram. Sci. Tech., 02 [03] 147-154 (2011)
DOI: 10.4416/JCST2011-00020
available online at: http://www.ceramic-science.com

2.75Yb-TZP Ceramics with High Strength and Aging Resistance

F. Kern*

University of Stuttgart, Institute for Manufacturing Technologies of Ceramic Components and Composites, 70569 Stuttgart, Allmandring 7 b, Germany

received 13 May, 2011; received in revised form 27 June, 2011; accepted 4 July, 2011

Abstract

Tetragonal zirconia polycrystals (TZP) ceramics for biomedical applications such as hip, knee or dental implants require good mechanical properties (hardness, toughness and strength) as well as low-temperature degradation (LTD) resistance. State-of-the-art Y-TZP and Ce-TZP do, however, suffer from deficiencies with regard to one of these aspects.

Shifting to other rare earth stabilizers may help solve this problem. 2.75Yb-TZP powder doped with 0.5 vol% alumina was produced from pyrogenic nanopowder via the nitrate route. Samples were produced by means of hot pressing at 1200 – 1400 °C for 1 h at 60 MPa axial pressure. Mechanical properties, phase composition and microstructure were investigated. LTD behaviour was examined with an accelerated aging test in an autoclave at 134 °C in water vapour. 2.75Yb-TZP has very high strength and hardness as well as moderate toughness. Degradation in water vapour is slight in the time frame relevant for implants.

Keywords: Zirconia, mechanical properties, microstructure, low-temperature degradation, ytterbia

I. Introduction

Excellent mechanical properties have made zirconia ceramics attractive for a multitude of mechanical and biomedical applications. A stress-induced martensitic transformation from tetragonal to monoclinic phase associated with volume expansion and shear sets the crack tip under compressive stress and thus slows or stops crack growth. Depending on the type of zirconia material, a combination of high strength and toughness can be achieved. [1] Tetragonal zirconia polycrystals (TZP) are most frequently stabilized with yttria or ceria. While Y-TZP has high strength, moderate toughness and negligible R-curve behaviour, Ce-TZP is extremely tough and flaw-tolerant, but its R-curve-dominated behaviour results in low bending strength. [2] A very interesting feature of Ce-TZP is its high resistance to LTD, conventional Y-TZP from co-precipitated powders has rather poor aging resistance especially if sintered to grain sizes > 0.5 µm. [3] It has been demonstrated that Y-TZP from coated powders shows improved aging resistance compared to Y-TZP from co-precipitated powder. [4,5] Coated powders are, however, no longer commercially available. In recent years the strategies to improve Y-TZP were the addition of alumina, the use of high stabilizer contents of 2.85 – 3.35 mol% and processing at low sintering temperatures (< 1400 °C). [6,7] Nanosized 3Y-TZP with grain sizes of ~100 nm shows almost unlimited aging resistance. However, strength and toughness were not improved in nano-3Y-TZP (σ_{4pt} = 922 MPa, $K_{IC,Anstis}$ = 3.9 MPa·$\sqrt{m}$) compared to standard material. [8] State-of-the-art alumina-doped 3Y-TZP processed at low temperature exhibits high strength (1 – 1.5 GPa) and hardness, but only very limited toughness (~5 MPa·$\sqrt{m}$) as the transformability is extremely low. [9]

Improvement of the strength of Ce-TZP can be achieved with the addition of alumina or hexaaluminate platelets. [10] The same effect was recently found for platelet-reinforced Y-TZP/alumina. [11]

One leading manufacturer of hip and knee implants has completely shifted to a zirconia-toughened alumina material of high strength, toughness and aging resistance to generally avoid the aging problems of Y-TZP. [12,13]

Recent investigations on TZP materials stabilized or co-stabilized with dopants other than yttria and ceria have shown the potential of rare earth stabilizers. Nd-Y-TZP has high toughness and attractive strength. [14,15] It was shown that co-precipitated Yb-TZP has improved toughness and strength compared to Y-TZP. [16] Y-Yb-TZP and Y-Gd-TZP were studied. [17] Some basic considerations indicate the stabilization with ytterbia may lead to more stable TZP and boost LTD performance. The ionic radius of Yb^{3+} is lower compared to that of Y^{3+}. Owing to the lanthanide contraction, the oxides of the lanthanides become less basic with rising atomic number, which may lead to higher hydrolytic stability. Less stabilizer may be required owing to the higher stability of the ytterbia-zirconia solid solution as indicated by the phase diagram. [18]

In this study an alumina-doped 2.75Yb-TZP material was produced from coated powder and characterized to validate these *a priori* assumptions.

* Corresponding author: frank.kern@ifkb.uni-stuttgart.de

II. Experimental

The coating process for zirconia powders via the nitrate route described by Yang was adapted to the pyrogenic nanopowders selected. [19, 5] 136.9 g of unstabilized zirconia VP-Ph (Evonik, Germany) with a crystallite size of 25 ± 2 nm and a specific surface area of 38.5 ± 3 m²/g and 0.5 g of α-alumina APA0.5 (d_{50} = 0.3 µm, S_{BET} = 8 m²/g, Ceralox, USA) was dispersed in 600 ml 2-propanol in a 1000-ml polyethylene bottle. 12.6 g of ytterbium oxide (99.9 % purity, Chempur, Germany) was dissolved in boiling half-concentrated nitric acid, cooled to room temperature and mixed with the zirconia dispersion. 600 g of 3Y-TZP milling balls (Ø = 5 mm) were added, then the dispersion was gently milled in the closed bottle for 12 h. After the milling balls had been separated, the mixed suspension was dried and the powder was heated to 250 °C to remove all remaining solvent. Then the mixture was ground with mortar and pestle and passed through a 125-µm screen. Then the screened powder was calcined at 800 °C for 30 min in air in an alumina crucible. The powder was attrition-milled in 2-propanol for 4 h at 500 rpm with the aim of reducing agglomeration. The resulting powder suspension was dried at 120 °C and screened through a 125-µm mesh.

Hot pressing (KCE, Germany) was performed in a boron-nitride-clad die of rectangular geometry (22.5 x 42.5 mm²). Two plates of 11.5 g were pressed simultaneously. The die was placed in the press, a pre-load of 2 MPa was applied and the furnace chamber was evacuated, then the press was heated at 50 K/min to 1150 °C, and the load was increased to 30 MPa. After 10 min precompaction the temperature was increased at 10 K/min to a final temperature of 1200 – 1400 °C (50 K increments). At final temperature the load was increased to 60 MPa for 1 h dwell. The samples were cooled in the press, with the heater shut off, in argon atmosphere.

Samples were prepared for characterization by lapping with 15-µm diamond suspension and subsequent polishing with 15-µm and 3-µm diamond suspension. The polished plates were each cut with a diamond wheel into seven bars of 4 mm in width for mechanical testing. Remaining pieces were kept for hardness testing and XRD.

Density was determined by means of immersion according to Archimedes. Vickers hardness HV_{10} (Bareiss, Germany) and microhardness $HV_{0.1}$ (Fischerscope, Germany) were measured. Indentation modulus was calculated from the loading-unloading curve of the microhardness measurement according to the universal hardness method. Bending strength was measured in a 3-pt setup according to DIN EN 6872 with 15-mm span. Fracture toughness was measured based on indentation strength in bending (ISB, according to Chantikul). A HV_{10} indent was placed in the middle of a bar, the indent was turned to the tensile side and the residual strength was determined. [20] Additionally indentation toughness was determined by means of direct crack length measurement according to Anstis. [21] The phase composition of polished, aged and fractured surfaces was investigated with XRD (Bruker Advance D8, CuKα, graphite monochromator). Monoclinic content was checked in the 27 – 33° 2θ-range by integrating the monoclinic (-111) and (111) and the tetragonal + cubic (101) reflexes and calculated according to the calibration curve of Toraya. [22] Cubic content was investigated in the 72.5 – 75° 2θ-range as described by Nakayama. [16]

Accelerated aging experiments in water vapour at 134 °C were performed in a small PTFE-clad stainless steel autoclave. Dwell times were 1, 3, 10, 30 and 100 h.

The microstructure of the samples was investigated with SEM (Jeol, Japan) on polished and thermally etched surfaces (1200 °C, 30 min, air). Images were taken in secondary electron mode at low acceleration voltage of 3 kV without conductive coating. The ytterbia-coated zirconia powder was examined by means of high-resolution SEM (Zeiss, Germany, SE Mode, 3kV). For this purpose, 500 mg of the milled powder was dispersed in 50 ml ethanol by means of ball milling followed by ultrasonic treatment. A drop of the suspension was put on a silicon wafer, dried and coated with platinum/palladium.

Surface roughness of the aged samples was checked with a tactile profilometer (Mahr, Germany). The surface structure of the aged specimens was investigated by means of light microscopy using differential interference contrast (DIC).

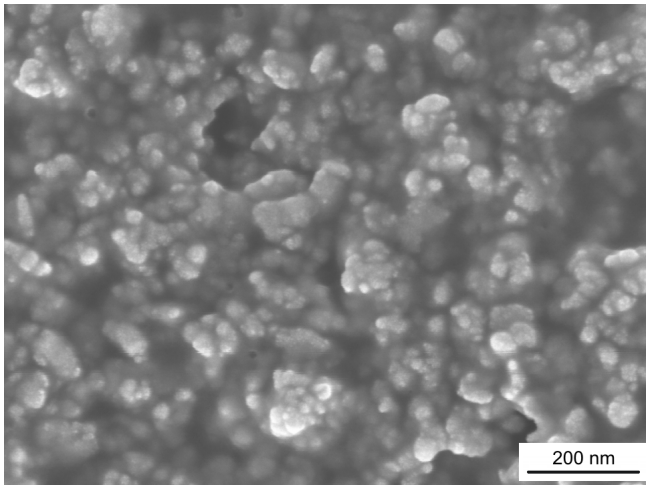

Fig. 1: High-resolution SEM image of the ytterbia-coated powder calcined at 800 °C.

III. Results and Discussion

For the VP-Ph nanozirconia powder a crystallite size of 25 ± 2 nm was determined by means of Scherrer analysis. As shown in an earlier investigation the unstabilized powder still contains a high fraction of tetragonal phase, which is a result of the pyrogenic production process and the fast quenching of the nanoparticles formed. [23] Compared to monoclinic zirconia of larger grain size, the reflexes are shifted to lower angles, which indicates some imperfections in the crystal structure. After powder coating and calcination at 800 °C, the instable tetragonal phase is completely eliminated. The size of the ytterbia crystallites formed after calcination can be estimated at 20 ± 2 nm with Scherrer analysis. A high-resolution SEM image (Fig. 1) shows that the ytterbia-coated powder consists of very small and not very well crystallized zirconia nanoparticles of 10 – 30 nm in size which are agglomerated. The size of the ytterbia crystallites is difficult to determine. Owing

to the higher mean atomic number, ytterbia should appear brighter than zirconia. In fact white dots on the surface of the zirconia particles are visible in the HR-SEM images, the size of these ytterbia crystallites (< 10 nm) is somewhat smaller than the value determined with XRD. Seemingly the stabilizer is not obtained as a coating but as homogeneously distributed nanoparticles. Grains in the dried suspension are very closely packed, making it difficult to determine the degree of hard agglomeration.

The Archimedes density of the specimen versus sintering temperature is shown in Table 1. The sintered specimen reaches a density of 6.25 – 6.26 g/cm³ at the lowest sintering temperature. This hints at a very fast diffusion process of ytterbia into the zirconia lattice and a complete formation of tetragonal phase. In Y-TZP a density increase from 1200 – 1250 °C can be observed. Ytterbia thus seems to diffuse faster than yttria and/or lead to more stable tetragonal phase at lower stabilizer concentration. Moreover the high density hints at a smaller lattice constant for coated 2.75Yb-TZP than for coated Y-TZP with the same stabilizer content. [5]

Table 1: Archimedes density of 2.75Yb-TZP versus sintering temperature

Sintering temperature [°C]	Density [g/cm³]	2 σ [g/cm³]
1200	6.2520	0.0080
1250	6.2555	0.0450
1300	6.2516	0.0229
1350	6.2616	0.0089
1400	6.2651	0.0198

Fig. 2 shows that the hardness of the 2.75Y-TZP materials produced is very high compared to literature data for Y-TZP (HV_{10} =1200 – 1350). Microhardness $HV_{0.1}$ shows a non-linear trend to decline slightly with rising sintering temperature, two hardness levels were observed 1600 ± 25 at 1200 °C and 1250 °C and 1575 ± 25 for the higher temperatures. Macrohardness also slightly declines from 1375 to 1350 HV_{10}.

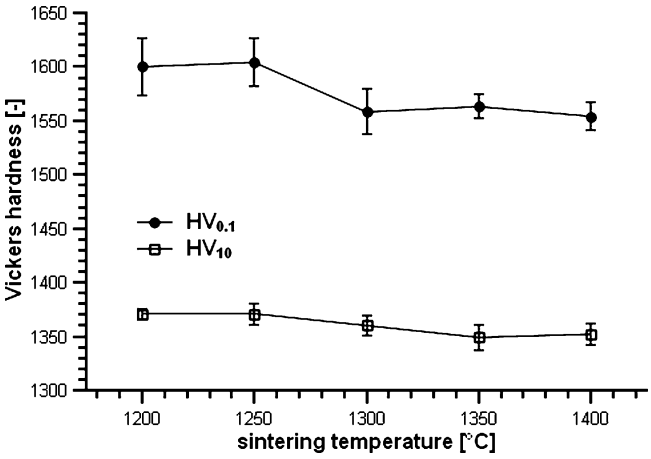

Fig. 2: Vickers hardness HV_{10} and $HV_{0.1}$ of 2.75Yb-TZP vs. sintering temperature.

The bending strength of 2.75Yb-TZP reaches the highest level of 1600 ± 200 MPa already at the lowest sintering temperature (Fig. 3). Then the strength declines and reaches its minimum level of 1350 MPa at 1300 °C. Strength rises again slightly to 1400 MPa at 1400 °C sintering temperature. The high strength level thus makes 2.75Yb-TZP very attractive for demanding structural applications. After an initial increase, the Young's modulus determined by indentation shows a maximum at a sintering temperature of 1250 °C, then falls with rising sintering temperatures. Indentation modulus values are approximately 10 % higher than the rule of mixture in transformation-toughened compounds. [5] This may be due to the phase transformation taking place during indentation, which induces compressive stresses leading to values that are systematically too high. The systematically too high Young's modulus also has some consequences for the fracture toughness measurements as the Young's modulus E is required for K_{IC} calculation. In the calculation formula for K_{IND} a factor $E^{0.5}$, in K_{ISB} a factor of $E^{0.125}$ is considered, corresponding to K_{IC} levels too high by ~ 5 % (K_{IND}) and ~ 1 % (K_{ISB}). Fig. 4 shows the fracture toughness of the materials sintered at different temperatures.

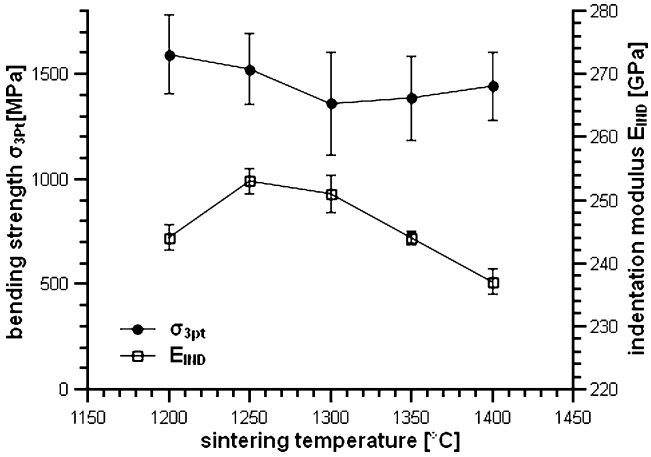

Fig. 3: 3-pt bending strength acc. DIN EN 6872 and indentation modulus of 2.75Yb-TZP vs. sintering temperature

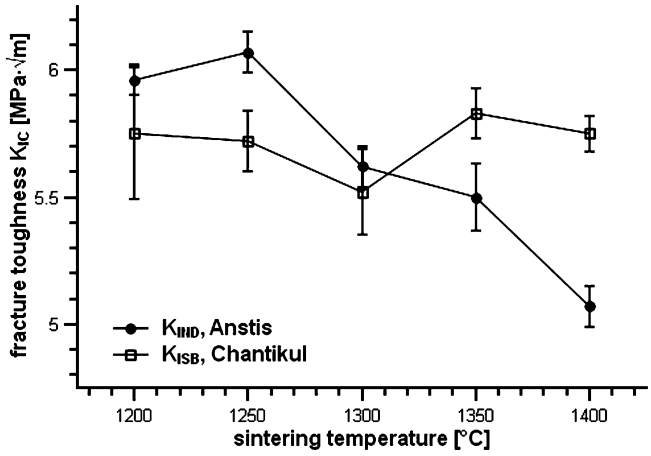

Fig. 4: Fracture toughness K_{IC} determined by means of direct crack length measurement (K_{IND}) and indentation strength in bending (K_{ISB}) of 2.75Yb-TZP vs. sintering temperature.

While the toughness K_{IND} according to Anstis determined with direct crack length measurement declines with rising sintering temperature from 6 to 5 MPa·$\sqrt{m}$, the toughness K_{ISB} determined with residual strength measurement stays at an almost constant level of 5.75 MPa·$\sqrt{m}$. Residual strength measured after a HV_{10} indent had an almost constant value of 360 – 370 MPa. Only a part of this mismatch between the methods may be due to the systematically too high Young's moduli.

Phase analysis can add some valuable information as we may conclude that the toughness increment added by transformation toughening will be approximately proportional to the fraction of tetragonal phase transformed.

Fig. 5 shows the results of the phase analysis of the polished surfaces and the fracture faces. The polished materials always seem to contain a fraction of 2 – 5 vol% monoclinic. Unfortunately the quantitative analysis of a few percent of monoclinic phase by XRD is rather tricky as it becomes difficult to correctly integrate the area of the small reflexes which hardly exceed the noise level. Thus the standard deviation is very high. Ohnishi suspected that the monoclinic content in the polished surfaces of Y-TZP produced from co-milled powders is introduced by the preparation process. [24] In the fracture faces the signal intensity is ten times lower than in polished surfaces owing to the higher roughness. The transformability of the tetragonal phase, calculated as the difference between the monoclinic content in fracture face and polished surface, ranges between 15 – 20 vol% with a high standard deviation of 5 – 10 vol%. The relatively constant transformability level rather confirms the toughness results based on the residual strength method.

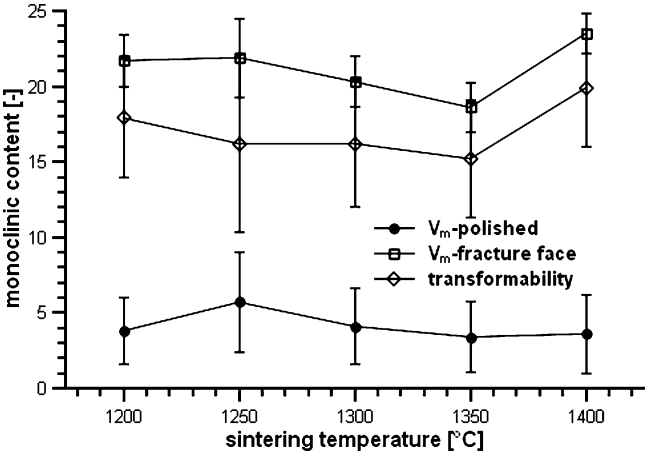

Fig. 5: Monoclinic content in polished and fractured 2.75Yb-TZP and transformability vs. sintering temperature.

The toughness level of 5.75 MPa·$\sqrt{m}$ is sufficiently high for e.g. dental implants (DIN EN 6872 requires 5 MPa·$\sqrt{m}$). Moreover the moderate toughness might be beneficial in tribological applications to avoid phase transformation during sliding contact.

The cubic content of the 2.75Yb-TZP was checked by means of XRD in the 72.5 – 75.5° 2θ-range. Fig. 6 shows that there is no clear indication of cubic phase. The $(400)_c$ reflex at 73.8° 2θ, if present at all, cannot be subtracted from the noise. We can see a reduction of line-broadening at higher sintering temperature and the formation of a clear doublet shape of the $(400)_t$ peak with proceeding grain growth. Nakayama found no cubic in 3Yb-TZP and 20 vol% cubic in 3.5 Yb-TZP. [16] From the phase diagram by Gonzalez we should, however, suspect some 10 vol% of cubic in the tested composition. Suppression of cubic phase formation may be a kinetic effect caused by the fast heating and moderate sintering temperatures. [18]

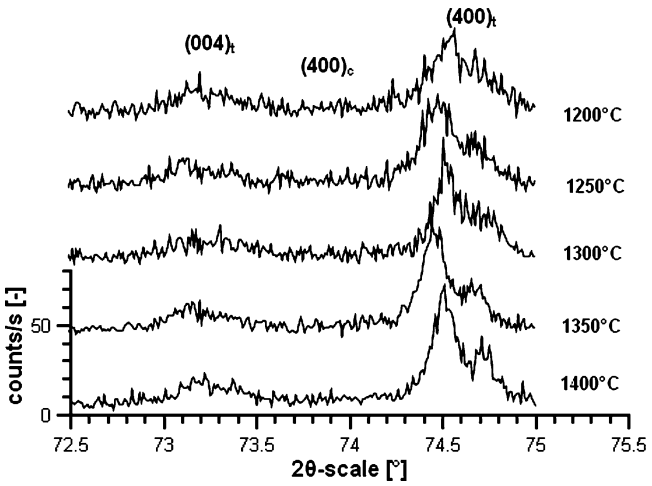

Fig. 6: XRD pattern of 2.75Yb-TZP sintered at 1200 – 1400 °C in the 72.5 – 75° 2θ-range.

The microstructure of 2.75Yb-TZP sintered at 1200, 1300 and 1400 °C and thermally etched at 1200 °C/30 min in air is shown in Fig. 7. The evolution of grain sizes with rising sintering temperature is shown in Fig. 8. The thermal etching temperature was kept very low in order not to induce additional grain growth. SEM images are thus slightly blurry as there is little etching induced topography in the surfaces. It is clearly visible that the grain size is initially very small (200 nm) and rises with increasing sintering temperature to a still moderate level of ~ 450 nm at maximum sintering temperature. Excessively large grains were not detected. Comparing the grain sizes with the toughness values we can observe no grain size dependence in toughness as in co-precipitated TZP. Besides grain growth as such, a certain broadening of the size distribution can be observed. The aging experiments conducted by means of exposition in water vapour at 134 °C for up to 100 h show some interesting details. All samples retained their structural integrity even after the highest exposition times. It was recently reported that in co-precipitated 3Y-TZP ceramics the aging resistance grows significantly with declining grain sizes. It was therefore expected to find the best results with the lowest sintering temperatures and grain sizes. Fig. 9, which plots the monoclinic content versus exposition time, shows, however, that samples sintered at 1200 and 1300 °C/h have similar aging characteristics. The sample sintered at 1400 °C ages faster. As the grain sizes of the samples sintered at 1300 °C and 1400 °C are very similar, the aging behaviour seems to be not only an issue of grain size but also of stabilizer distribution gradient. With increasing sintering temperature we can expect the ytterbia concentration to equilibrate while at low sintering temperatures a certain concentration gradient from the shell to the core of the individual grains is present. The surface roughness R_a plotted versus

aging time (Fig. 10) shows a similar tendency. The materials sintered at 1300 °C and 1400 °C are relatively stable up to exposition times of 10 h, between 10 h and 30 h aging time at 134 °C the roughness begins to increase. The sample sintered at 1200 °C is even stable up to 30 h, then the roughness increases. Considering the typical activation energies (106 KJ/mol) for the aging processes of Y-TZP determined by Chevalier, it is possible to extrapolate the results of the accelerated aging tests to lower aging temperatures. [25] The model has been recently confirmed and is the basis for the existing standard for assessment of biomedical implants (ISO 13356). [26] Taking into account that the phase transformation and the surface roughening are moderate up to aging times of 10 h, the material can be considered safe for implant materials with *in vivo* residence times of 25 – 35 years. Images of the aged surfaces taken with digital interference contrast microscopy show increasing corrugation of the surface of the 2.75Yb-TZP ceramic sintered at 1300 °C/1 h with increasing aging time (Fig. 12). Evidently this is caused by low-temperature degradation and nucleation and growth of monoclinic crystallites. Information from microscopy is in accord with roughness measurements and phase analysis. 2.75Yb-TZP stays stable for at least 10 h before the surface begins to roughen. The coefficients of Mehl-Avrami-Johnson (MAJ) kinetics (Eq. 1) were determined according to a procedure previously reported by Chevalier. [25]

$$f = s \cdot e(-b \cdot t)^n \quad (1)$$

f = monoclinic content	[-]
s = maximum transformability (88%)	[-]
b = rate constant	[h^{-1}]
t = time	[h]
n = Avrami exponent	[-]

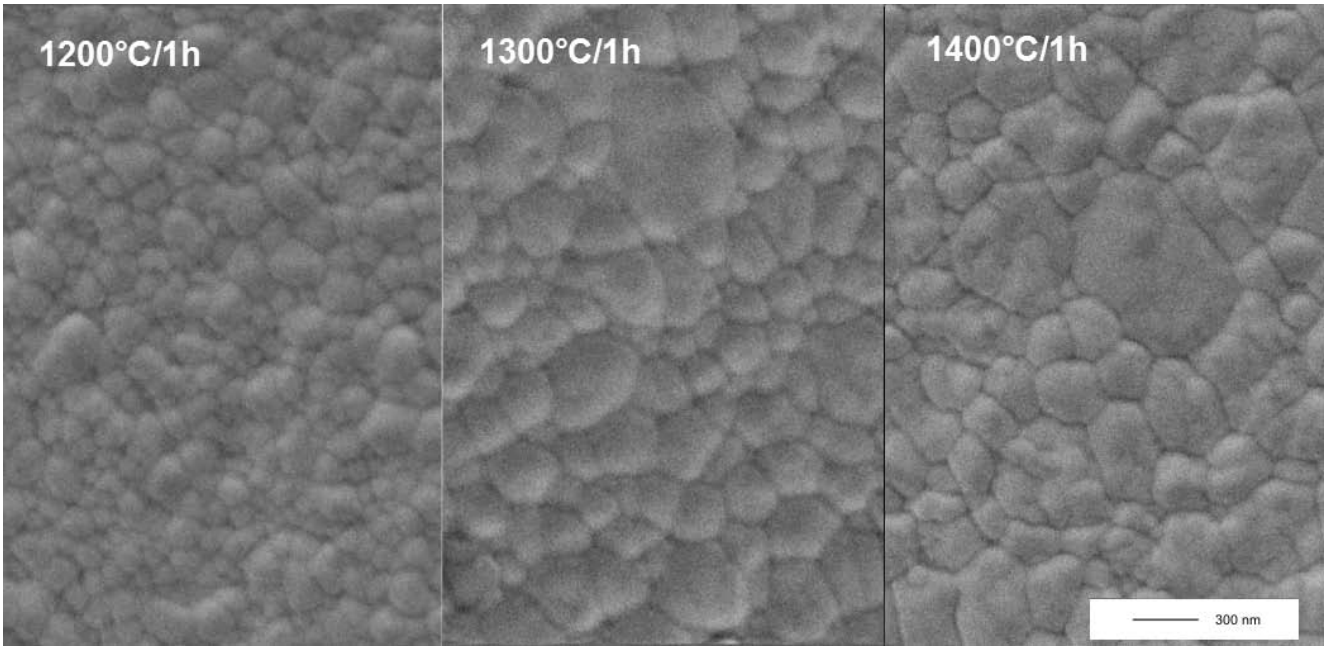

Fig. 7: SEM image of the microstructure of 2.75Yb-TZP sintered at 1200, 1300 and 1400 °C (polished and thermally etched 1200 °C/30 min/air).

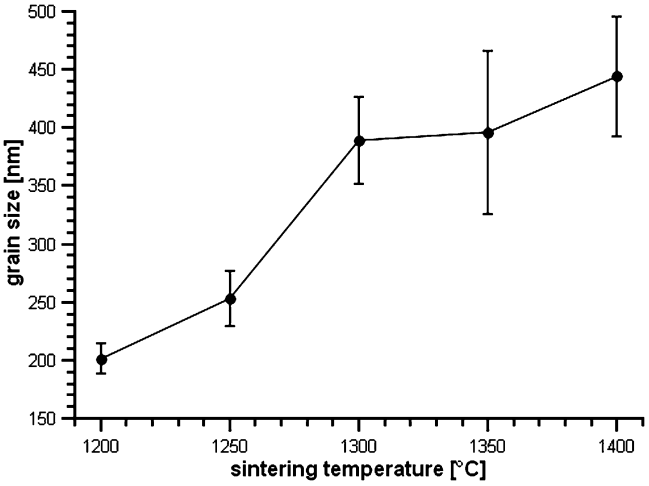

Fig. 8: Grain size of 2.75Yb-TZP determined by line intercept method vs. sintering temperature.

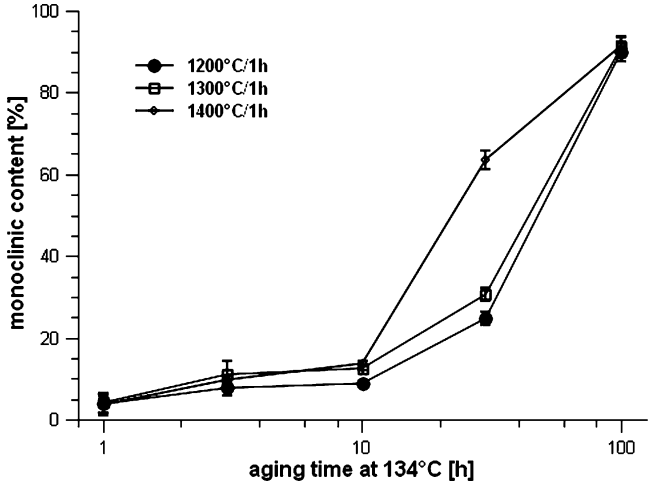

Fig. 9: Monoclinic content in 2.75Yb-TZP samples sintered at 1200, 1300 and 1400 °C vs. aging time at 134 °C in autoclave test.

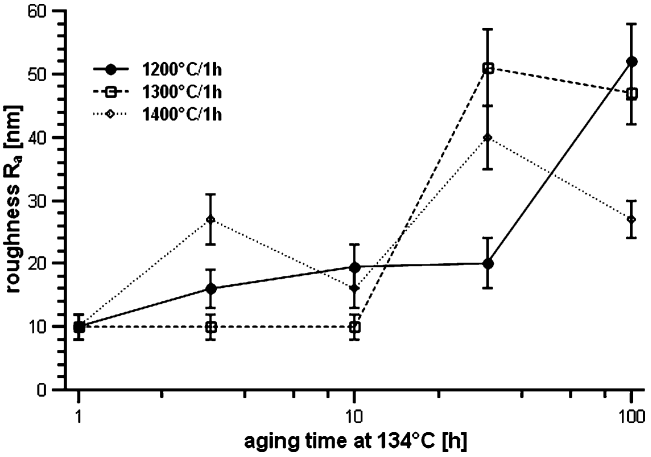

Fig. 10: Surface roughness 2.75Yb-TZP vs aging time at 134 °C in autoclave test.

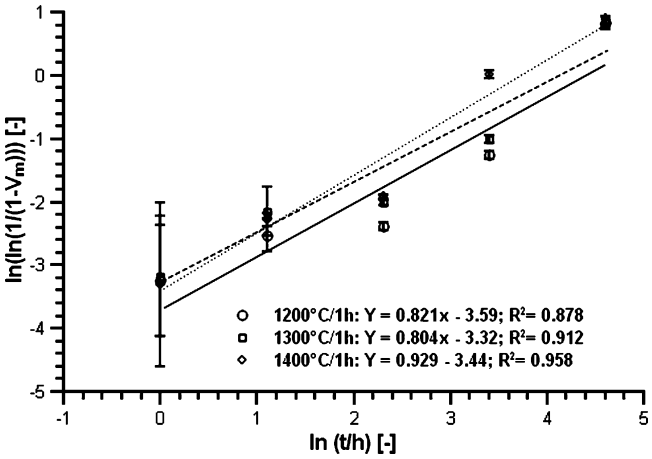

Fig. 11: Coefficients of the Mehl-Avrami-Johnson nucleation and growth kinetics determined on samples sintered at 1200, 1300 and 1400 °C and aged for up to 100 h.

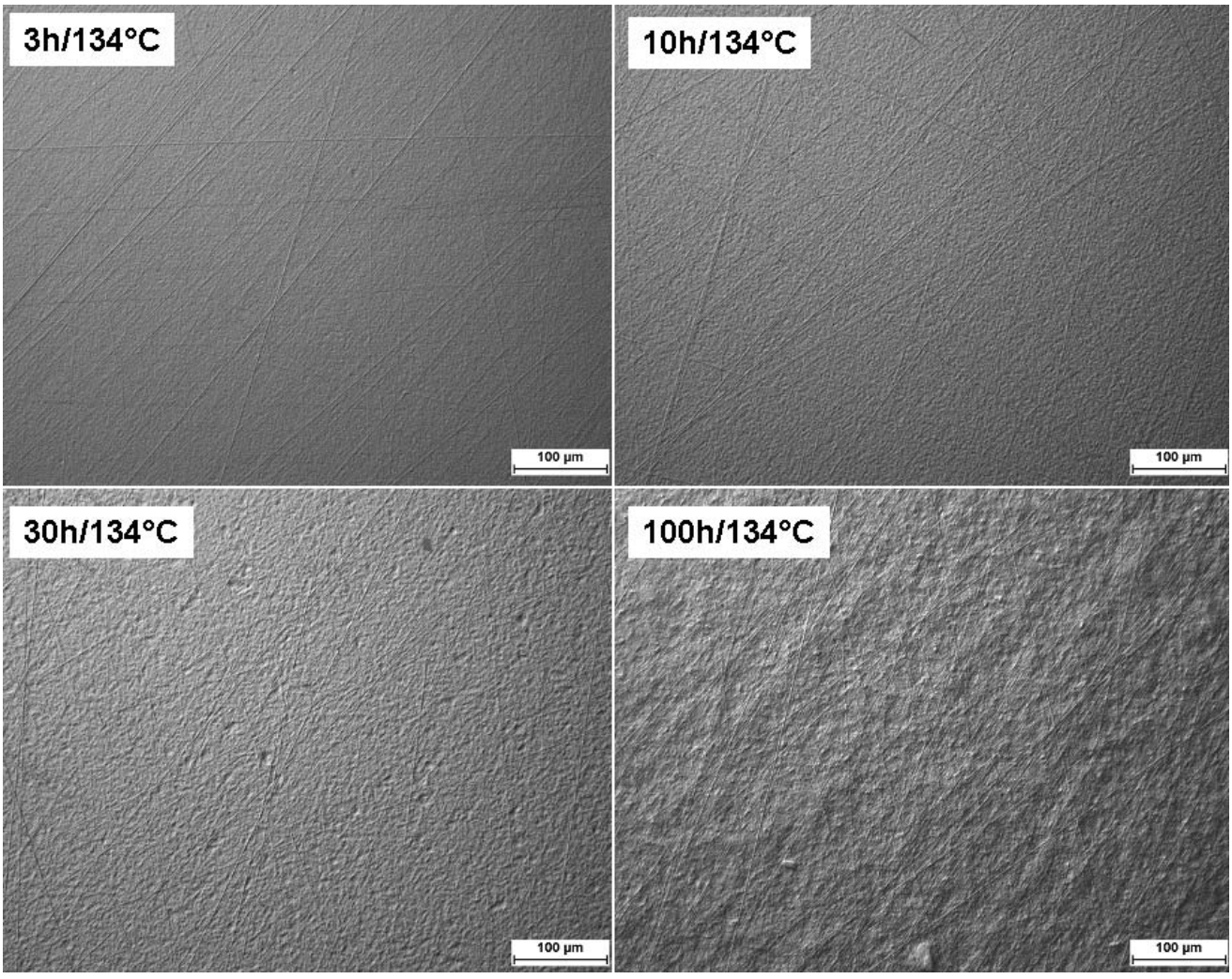

Fig. 12: Microscopy images taken with differential interference contrast (DIC) of 2.75Yb-TZP sintered at 1300 °C vs. aging times of 3, 10, 30 and 100 h.

The Avrami exponents and rate constants determined are shown in Fig. 11. Avrami exponents – defined by the slope of the linear regression – are rather low (n = 0.8 – 0.96) compared to literature data for co-precipitated Y-TZP. [25] A closer look at the data points shows that at short aging times the Avrami exponents are even lower (~ 0.5) while at longer aging times exceeding 10 h the exponents are closer to n = 2 – 3. Similar behaviour was recently found for Y-TZP from coated nanopowder. [5] The y-axis intercept of the regression lines is the natural logarithm of the rate constant b (ln (b) = -3.3 to -3.6). The rate constants are much lower than literature data (ln(b) = -2 to -2.5), indicating that transformation in 2.75Yb-TZP proceeds more slowly by a factor of 3 – 4 than in co-precipitated Y-TZP. [25] Re-

sults obtained at 1 h of aging should not be overstressed owing to the systematically high standard deviations at short aging times.

IV. Summary and Conclusion

2.75Yb-TZP ceramics derived from ytterbia-coated pyrogenic zirconia nanopowder were produced by means of hot pressing. The materials obtained show very high mechanical strength and hardness and fracture toughness superior to co-precipitated 3Y-TZP. The ceramics are very fine-grained (200 – 450 nm). The investigation of their phase composition shows no indication of cubic phase formation, the transformability of the 2.75Yb-TZP is moderate. The aging resistance of the 2.75Yb-TZP material is very good compared to standard co-precipitated 3Y-TZP, moreover the phase transformation does not destroy the samples even at long exposition times. Recent developments in nano-3Y-TZP have focused on materials with unlimited aging stability, this also implicates that transformability and thereby toughness and bending strength are limited. In 2.75Yb-TZP a good balance between mechanical properties and sufficient low-temperature degradation stability was found, which qualifies 2.75Yb-TZP for demanding mechanical engineering and tribological applications as well as for biomedical implants. In order to verify this statement, the coming challenge will be to translate the results of this material-science-related study to real components. This will require the choice of a different starting powder with better processability, a scale-up of the powder coating process and the shaping, sintering and testing of components.

References

1 Hannink, R.J., Kelly, P.M., Muddle, B.C.: Transformation toughening in zirconia-containing ceramics, *J. Am. Ceram. Soc.*, **83**, [3], 461 – 87, (2000).

2 Swain, M.V., Rose, L.R.F.: Strength limitations in transformation-toughened zirconia alloys, *J. Am. Ceram. Soc.*, **69**, [7], 511 – 18, (1986).

3 Marro, F.G., Valle, J., Mestra, A., Anglada, M.: Surface modification of 3Y-TZP with cerium oxide, *J. Eur. Ceram. Soc.*, **31**, [3], 331 – 338, (2011).

4 Picconi, C., Burger, W.. Richter, H.G., Cittadini, A., Maccauro, G., Covacci, V., Bruzzese, N., Ricci, G.A., Marmo, E.: Y-TZP ceramics for artificial joint replacements, *Biomaterials*, **19**, 1489 – 1494, (1998).

5 Kern, F.: Alumina-doped 2.5Y-TZP produced from yttria-coated pyrogenic Nanopowder", *J. Ceram. Sci. Tech.*, **2**, [2], 89 – 96, (2011).

6 Matsui, K., Yoshida, H., Ikuhara, Y.: Phase-transformation and grain-growth kinetics in yttria-stabilized tetragonal zirconia polycrystal doped with a small amount of alumina, *J. Eur. Cer. Soc.,* **30**, [7], 1679 – 1690, (2010).

7 Tsubakino, H., Sonoda, K., Nozato, R.: Martensite transformation behaviour during isothermal ageing in partially stabilized zirconia with and without alumina addition, *J. Mat. Sci. Let.*, **12**, 196 – 198, (1993).

8 Binner, J., Vaidhyanathan, B., Paul, A., Annaporani, K., Raghupathy, B.: Compositional effects in nanostructured yttria partially stabilized zirconia, *J. Appl. Cer. Techn.*, **8**, [3], DOI: 10.1111/j.1744 – 7402.2010.02503.x, (2011).

9 Begand, S., Oberbach, T., Glien, W.: Tribological behaviour of an alumina-toughened zirconia ceramic for an application in joint prosthesis, *Key Eng. Mater.*, 309 – 311, 1261 – 1264, (2006).

10 Cutler, R.A., Mayhew, R.J., Pr*etty*man, K.M. and Virkar, A.V.: High-toughness Ce-TZP/Al_2O_3 ceramics with improved hardness and strength, *J. Am. Ceram. Soc.*, **74**, [1], 179 – 86, (1991).

11 Kern, F.. Gadow, R.: Influence of *In-Situ* platelet reinforcement on the properties of injection-molded alumina-toughened zirconia, *J. Ceram. Sci. Tech.*, **2**, [1], 47 – 54, (2011).

12 Burger, W., Richter, H.G.: High-strength and toughness alumina matrix composites by transformation toughening and *In Situ* platelet reinforcement (ZPTA) – the new generation of bioceramics, *Key Eng. Mat.*, 192 – 195, 545 – 548, (2001).

13 Chevalier, J., Grandjean, S., Kuntz, M., Pezzotti, G.: On the kinetics and impact of tetragonal to monoclinic transformation in an Alumina/Zirconia composite for arthroplasty applications, *Biomaterials*, **30**, [29], 5279 – 5282, (2009).

14 Xu, T., Vleugels, J., Van der Biest, O., Wang, P.: Mechanical properties of Nd_2O_3/Y_2O_3-coated zirconia ceramics, *Mat. Sci.Eng. A*, **374**, 239 – 234, (2004).

15 Vleugels, J., Xu, T., Huang, S., Kan, Y., Wang, P., Li, L., Van der Biest, O: Characterization of (Nd,Y)-TZP ceramics prepared by a colloidal suspension coating technique, *J. Eur. Ceram. Soc.*, **27**, 1339 – 43, (2007).

16 Nakayama, S., Maekawa, S., Sato, T., Masuda, Y., Imai, S., Sakamoto, M.: Mechanical properties of ytterbia-stabilized zirconia ceramics (Yb-TZP) fabricated from powders prepared by co-precipitation method, *Ceram. Int.*, **26**, 207 – 211, (2000).

17 Kan, Y., Li, S., Wang, P., Zhang, G., Van der Biest, O., Vleugels, J.: Preparation and conductivity of Yb_2O_3-Y_2O_3 and Gd_2O_3-Y_2O_3 co-doped zirconia ceramics, *Solid State Ionics*, **179**, 1531 – 1534, (2004).

18 Gonzalez, M., Moure, C., Jurado, J.R., Duran, P.: Solid-state reaction, microstructure and phase relations in the ZrO_2-rich region of the ZrO_2-Yb_2O_3 system, *J. Mat. Sci.*, **28**, 3451 – 3456, (1993).

19 Yuan, Z.X., Vleugels, J., Van der Biest, O.: Preparation of Y_2O_3-coated ZrO_2 powder by suspension drying, *J. Mat. Sci. Let.*, **19**, 359 – 361, (2000).

20 Chantikul, P., Anstis, G.R., Lawn, B.R., Marshall, D.B.: A critical evaluation of indentation techniques for measuring fracture Toughness: II, strength method, *J. Am. Ceram. Soc.*, **64**, [9], 539 – 543, (1981).

21 Anstis, G.R., Chantikul, P., Lawn, B.R., Marshall, D.B.: A critical evaluation of indentation techniques for measuring fracture Toughness: I, direct crack measurements, *J. Am. Ceram. Soc.*, **64**, [9], 533 – 538, (1981).

22 Toraya, H., Yoshimura, M., Somiya, S.: Calibration curve for quantitative analysis of the monoclinic-tetragonal ZrO_2 system by X-ray diffraction, *J. Am. Ceram. Soc.*, **67**, [6], C119 – 121, (1984).

23 Kern, F: 2.5Y-TZP from yttria-coated pyrogenic zirconia nanopowder, *J. Ceram. Sci. Tech.*, **1**, [1], 21 – 26, (2010).

24 Ohnishi, H., Naka, H., Sekino, T., Ikuhara, Y., Niihara, K.: Mechanical properties of 2.0 – 3.5 mol% Y_2O_3-stabilized zirconia polycrystals fabricated by the solid phase mixing and sintering method, *J. Ceram. Soc. Jap.*, **116**, 1360, 1270 – 1277, (2008).

25 Chevalier, J., Cales, B., Drouin, J-M.: Low-temperature ageing of Y-TZP ceramics, *J. Am. Ceram. Soc.*, **82**, [8], 2150 – 54, (1999).

26 Chevalier, J., Grandjean, S., Kuntz, M., Pezzotti, G.: Activation energy for Polymorphic transformation in an advanced Alumina/Zirconia composite for arthroplastic applications, *Biomaterials*, **30**, 5279 – 82, (2009)